

COVID-CT-Dataset: A CT Image Dataset about COVID-19

Jinyu Zhao*

UC San Diego

JIZ077@ENG.UCSD.EDU

Xuehai He*

UC San Diego

X5HE@ENG.UCSD.EDU

Xingyi Yang*

UC San Diego

X3YANG@ENG.UCSD.EDU

Yichen Zhang

UC San Diego

YIZ037@ENG.UCSD.EDU

Shanghang Zhang

UC Berkeley

SHZ@EECS.BERKELEY.EDU

Pengtao Xie

UC San Diego

PENGTAOXIE2008@GMAIL.COM

Abstract

During the outbreak time of COVID-19, computed tomography (CT) is a useful manner for diagnosing COVID-19 patients. To mitigate the lack of publicly available COVID-19 CT images for developing CT-based diagnosis deep learning models of COVID-19, we build an open-sourced dataset COVID-CT, which contains 349 COVID-19 CT images from 216 patients and 463 non-COVID-19 CTs. The utility of this dataset is confirmed by a senior radiologist and via experimental studies. Using this dataset, we develop a joint classification and segmentation method that achieves an F1 of 0.85, an AUC of 0.95, and an accuracy of 0.83. The data and code are available at <https://github.com/UCSD-AI4H/COVID-CT>

1. Introduction

Coronavirus disease 2019 (COVID-19) is an infectious disease that has caused 279,321 deaths all over the world, among 4,024,973 infected cases, as of May 9, 2020. One major hurdle in controlling the spreading of this disease is the shortage of tests. The current tests are mostly based on reverse transcription polymerase chain reaction (RT-PCR). During the peak time of COVID-19 outbreak, RT-PCR test kits are in great shortage. As a result, many suspected cases cannot be tested in time and they continue to spread the disease unconsciously. To mitigate the shortage of RT-PCR test kits, hospitals have been utilizing alternative diagnosis methods. Among them, computed tomography (CT) scans have been used for screening and diagnosing COVID-19. For example, in the Diagnosis and Treatment Protocol for Novel Coronavirus Pneumonia (Trial Version 5)¹ made by the National Health Commission and State Administration of Traditional Chinese Medicine in China, CT and other chest imaging techniques have been named as an important way for

0. *Equal contribution

1. http://www.kankyokansen.org/uploads/uploads/files/jsipc/protocol_V5.pdf

diagnosing COVID-19. Following this guideline, many hospitals in China used CT scans for COVID-19 diagnosis, which has been demonstrated to be effective.

To further understand the role of CT in diagnosing COVID-19, we consulted a senior radiologist in Tongji Hospital, Wuhan, China, who has been diagnosing and treating COVID-19 patients since the outbreak of this disease in China starting from January. According to this radiologist, during the outbreak time, CT is useful in diagnosing COVID-19; out of the outbreak time, CT is not as useful. The reasons are as follows. CTs can be used to judge whether a patient is infected by viral pneumonia (COVID-19 is a type of viral pneumonia caused by the SARS-CoV-2 virus). However, CTs do not have the ability to determine which virus is causing the viral pneumonia: SARS-CoV-2 or others. Strictly speaking, CTs cannot be used to confirm whether a patient is infected by COVID-19. However, during the outbreak time, most viral pneumonia is caused by SARS-CoV-2. That is to say, if a patient is diagnosed with viral pneumonia by CT, this viral pneumonia is very likely to be COVID-19. Due to this fact, CT is useful in diagnosing COVID-19 during the outbreak time.

During the outbreak of COVID-19, radiologists are highly occupied, who may not have the bandwidth to read a number of CT scans timely. Besides, for radiologists in under-developed areas, such as rural regions, they may not be well-trained to recognize COVID-19 from CT scans, since this disease is relatively new. To address these problems, several works (Huang et al., 2020; Li et al., 2020) have developed deep learning methods to screen COVID-19 from CTs. Due to privacy concerns, the CT scans used in these works are not shared with the public. This greatly hinders the research and development of more advanced AI methods for more accurate screening of COVID-19 based on CT.

To address this issue, we build a COVID-CT dataset which contains 349 CT images positive for COVID-19 and 397 CT images that are negative for COVID-19 and is open-sourced to the public, to foster the R&D of CT-based testing of COVID-19. From 760 medRxiv and bioRxiv preprints about COVID-19, we extract reported CT images and manually select those containing clinical findings of COVID-19 by reading the captions of these images. After releasing this dataset, we received several feedback expressing concerns about the usability of this dataset. The major concerns are summarized as follows. First, when the original CT images are put into papers, the quality of these images are degraded, which may render the diagnosis decisions less accurate. The quality degradation includes: the Hounsfield unit (HU) values are lost; the number of bits per pixel is reduced; the resolution of images is reduced. Second, the original CT scan contains a sequence of CT slices, but when put into papers, only a few key slices are selected, which may have a negative impact on diagnosis as well.

We consulted the aforementioned radiologist at Tongji Hospital regarding these two concerns. According to the radiologist, the issues raised in these concerns do not significantly affect the accuracy of diagnosis decision-making. First, experienced radiologists are able to make accurate diagnosis from low quality CT images. For example, given a photo taken by smart phone of the original CT image, experienced radiologists can make accurate diagnosis by just looking at the photo, though the CT image in the photo has much lower quality than the original CT image. Likewise, the quality gap between CT images in papers and original CT images will not largely hurt the accuracy of diagnosis. Second, while it is preferable

to read a sequence of CT slices, oftentimes a single-slice of CT contains enough clinical information for accurate decision-making.

To further address these concerns, we use the CT images extracted from papers for model training only. For testing, we use original CT images donated by hospitals. Validation is also conducted on original CTs. We compare models trained on our paper-extracted CTs and models trained on original CTs, and the former outperforms the latter. This demonstrates that COVID-19 CTs extracted from papers are useful for training diagnosis models of COVID-19. In the end, we leverage our COVID-CT dataset, original CT images collected elsewhere, lesion masks labeled by radiologists to train a diagnosis model of COVID-19, based on multi-task learning. This model achieves an F1 score of 84.6%, an accuracy of 83.3%, and an AUC of 94.8%.

The rest of the paper is organized as follows. In Section 2, we introduce the COVID-CT dataset. In Section 3, we perform a study to verify whether COVID-CT is useful for training COVID-19 diagnosis models. In Section 4, we develop a multi-task learning model to improve the diagnosis accuracy of COVID-19. Section 5 concludes the paper.

2. The COVID-CT Dataset

In this section, we describe how the COVID-CT dataset is built. We first collected 760 preprints about COVID-19 from medRxiv² and bioRxiv³, posted from Jan 19th to Mar 25th. Many of these preprints report patient cases of COVID-19 and some of them show CT images in the reports. CT images are associated with captions describing the clinical findings in the CTs. We used PyMuPDF⁴ to extract the low-level structure information of the PDF files of preprints and located all the embedded figures. The quality (including resolution, size, etc.) of figures are well-preserved. From the structure information, we also identified the captions associated with figures. Given these extracted figures and captions, we first manually select all CT images. Then for each CT image, we read the associated caption to judge whether it is positive for COVID-19. If not able to judge from the caption, we located the text analyzing this figure in the preprint to make a decision. For each CT image, we also collect the meta information extracted from the paper, such as patient age, gender, location, medical history, scan time, severity of COVID-19, and radiology report. For any figure that contains multiple CT images as sub-figures, we manually split it into individual CTs, as shown in Figure 1.

2. <https://www.medrxiv.org/>

3. <https://www.biorxiv.org/>

4. <https://github.com/pymupdf/PyMuPDF>

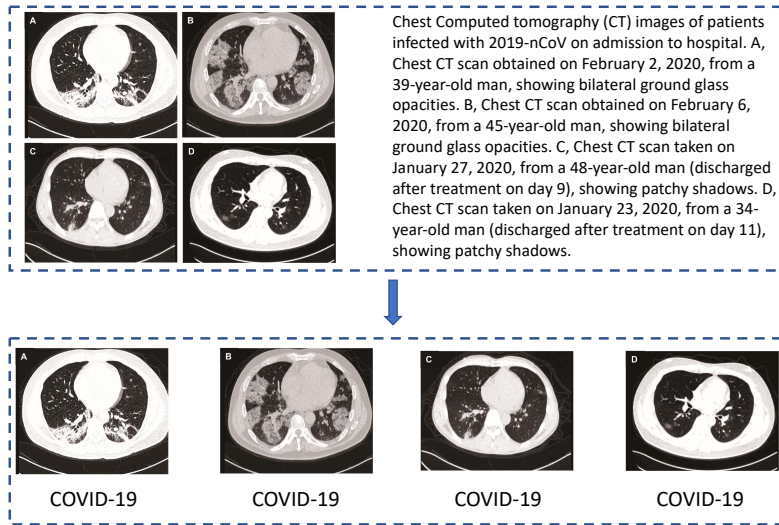


Figure 1: For any figure that contains multiple CT images as sub-figures, we manually split it into individual CTs.

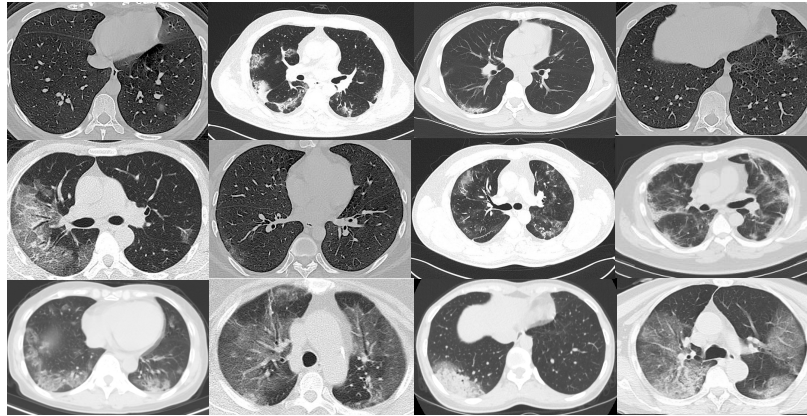


Figure 2: Examples of CT images that are positive for COVID-19.

In the end, we obtain 349 CT images labeled as being positive for COVID-19. These CT images have different sizes. The minimum, average, and maximum height are 153, 491, and 1853. The minimum, average, and maximum width are 124, 383, and 1485. These images are from 216 patient cases. Figure 2 shows some examples of the COVID-19 CT images. For patients labeled with positive, 169 of them have age information and 137 of them have gender information. Figure 3 shows the age distribution of patients with COVID-19. Figure 4 shows the gender ratio of patients with COVID-19. Male patients are more than female patients, with a number of 86 and 51 respectively.

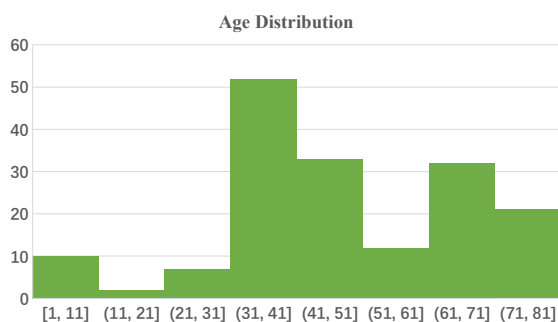


Figure 3: Age distribution of COVID-19 patients

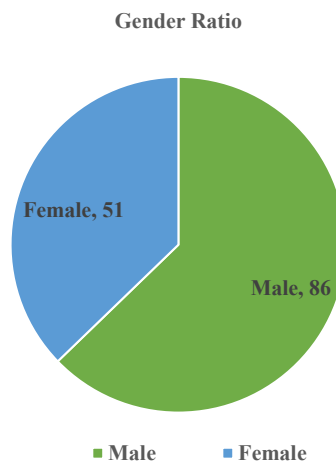


Figure 4: The gender ratio of COVID-19 patients. The ratio of male:female is 86:51.

Collection of non-COVID-19 CT images as negative training set To develop binary classification models for diagnosing COVID-19, in addition to the 349 COVID-19 CT images, we also collect a set of non-COVID-19 CT images. The sources of these images include:

- The MedPix⁵ database, which is an open-access online database of medical images, teaching cases, and clinical topics. It contains more than 9000 topics, 59000 images from 12000 patient cases.
- The LUNA⁶ dataset, which contains 888 lung cancer CT scans from 888 patients.
- The Radiopaedia website⁷, which contains radiology images from 36559 patient cases.
- PubMed Central (PMC)⁸, which is a free full-text archive of biomedical and life sciences journal literature.

Table 1: Statistics of the negative training set

	Class	LUNA	MedPix	PMC	Radiopaedia	Total
# patients	Non-COVID	17	✗	✗	2	✗
# images	Non-COVID	36	195	202	30	463

Table 2 shows the composition of the negative training set which contains 463 images: 36 from LUNA, 195 from MedPix, 202 from PMC, and 30 from Radiopaedia.

5. <https://medpix.nlm.nih.gov/home>
 6. <https://luna16.grand-challenge.org/>
 7. <https://radiopaedia.org/articles/covid-19-3>
 8. <https://www.ncbi.nlm.nih.gov/pmc/>

Table 2: Statistics of the test set

	Class	LUNA	COVID-Seg	Radiopaedia	Total
# patients	COVID	0	4	0	4
	Non-COVID	19	0	1	20
# images	COVID	0	173	0	173
	Non-COVID	164	0	4	168

Table 3: Statistics of the validation set

	Class	LUNA	COVID-Seg	Radiopaedia	Total
# patients	COVID	0	4	0	4
	Non-COVID	38	0	1	39
# images	COVID	0	88	0	88
	Non-COVID	48	0	16	64

Collection of test and validation images To evaluate the trained models, we collect a validation set and a test set. In these two sets, all images are original CTs donated by hospitals. None of them is extracted from papers.

The sources of original COVID-19 CTs include:

- The COVID-19 CT Segmentation Dataset (COVID-Seg)⁹, which contains 20 axial volumetric COVID-19 CT scans.

The sources of original non-COVID-19 CTs include:

- The LUNA¹⁰ dataset, which contains 888 lung cancer CT scans from 888 patients.
- The Radiopaedia website¹¹, which contains radiology images from 36559 patient cases.

Table 2 shows the composition of the test set. It has 173 COVID-19 CT images, from 4 patients in the COVID-Seg dataset. It contains 168 non-COVID-19 CT images: 164 of them are from 19 patients in the LUNA dataset and the rest 4 are from 1 patient in Radiopaedia. Table 3 shows the composition of the validation set. It has 88 COVID-19 CT images, from 4 patients in the COVID-Seg dataset. It contains 64 non-COVID-19 CT images: 48 of them are from 38 patients in the LUNA dataset and the rest 16 are from 1 patient in Radiopaedia. The images from LUNA are either about lung cancer or normal. The images from Radiopaedia are normal. We automatically crop the chest position in images through threshold segmentation and convex hull detection, which gets rid of white space at the edge of images.

3. Study: Is COVID-CT useful for training CT-based diagnosis models of COVID-19?

As mentioned before, we received several feedback expressing concerns that the COVID-CT dataset may not be useful for training CT-based diagnosis models for COVID-19 since (1)

9. <http://medicalsegmentation.com/covid19/>

10. <https://luna16.grand-challenge.org/>

11. <https://radiopaedia.org/articles/covid-19-3>

images in COVID-CT are extracted from papers in PDF format, which are likely to have lower quality compared with original CT scans and (2) images in COVID-CT are single-slice CTs rather than multiple-slice CTs as in original CT scans. In this section, we perform an experimental study to investigate whether the images in COVID-CT are useful in training CT-based diagnosis models.

Study Design We compare experimental settings with three different positive training datasets.

- **COVID-Seg:** We use 118 positive CTs in COVID-Seg as positive training examples. These images are original CT images obtained from the image archiving systems in hospitals.
- **COVID-CT-349:** We use the full set of 349 COVID-19 CTs in COVID-CT as positive training examples. These images are extracted from papers.
- **COVID-CT-118:** We randomly sample 118 images from COVID-CT as positive training examples. These images are extracted from papers.

The negative training images, test images, and validation images are the same for the above-mentioned three settings, as given in Table 1, 2, and 3 respectively. The images used for validation and testing are original CT images obtained from the image archiving systems in hospitals. We use the DenseNet-169 (Huang et al., 2017) model for classifying a CT image as COVID-19 or non-COVID-19. It is pretrained on the ImageNet (Deng et al., 2009) dataset. The trained models are evaluated using three metrics: accuracy, F1, and area under ROC curve (AUC). For all metrics, the higher the better. Hyperparameters are tuned on the validation set.

Experimental Settings Input images are resized to 480-by-480. We perform data augmentation on the training set. Each training image is augmented with random cropping with a scale of 0.5, horizontal flip, random contrast, and random brightness with a factor of 0.2. The weight parameters in the networks are optimized using Adam (Kingma and Ba, 2014) with an initial learning rate of 0.0001 and a mini-batch size of 16. Cosine scheduling with a period of 10 is used to adjust the learning rate across the training process. We implement the network using PyTorch and train it on one GTX 1080Ti GPU.

Results Table 4 shows the results on the test set, under three settings of positive training images. From this table, we observe the following. First, the model trained on COVID-CT-349 is largely better than that trained on COVID-Seg. COVID-CT-349 contains images extracted from papers. COVID-Seg contains original CT images. This demonstrates that COVID-CT is useful for training CT-based diagnosis models for COVID-19, despite the concerns that images extracted from papers have low quality and are single slices. Second, the model trained on COVID-CT-349 is much better than that trained on COVID-CT-118. Adding more COVID-CT images into the training set substantially improves performance, which further demonstrates that the CTs in COVID-CT have high utility in training COVID-19 diagnosis models. Third, COVID-Seg outperforms COVID-CT-118. These two sets have the same number of images. This indicates that original CTs are more useful for model training than images extracted from papers. In sum, these results demonstrate the usefulness of our COVID-CT dataset in training diagnosis models.

Positive training data	Accuracy (%)	F1-score (%)	AUC (%)
COVID-Seg	64.8	50.0	79.5
COVID-CT-349	79.5	76.0	90.1
COVID-CT-118	57.8	36.3	75.2

Table 4: Performance of DenseNet-169 on the test set under different settings of positive training images.

4. Study II: How to improve the performance to a clinically more useful level?

In the previous study, we have shown that COVID-CT is useful for model training and achieves much better performance than purely using original COVID-19 CT images. But the accuracy is still low. In this section, we develop a method that improves the diagnosis accuracy to a clinically more useful level.

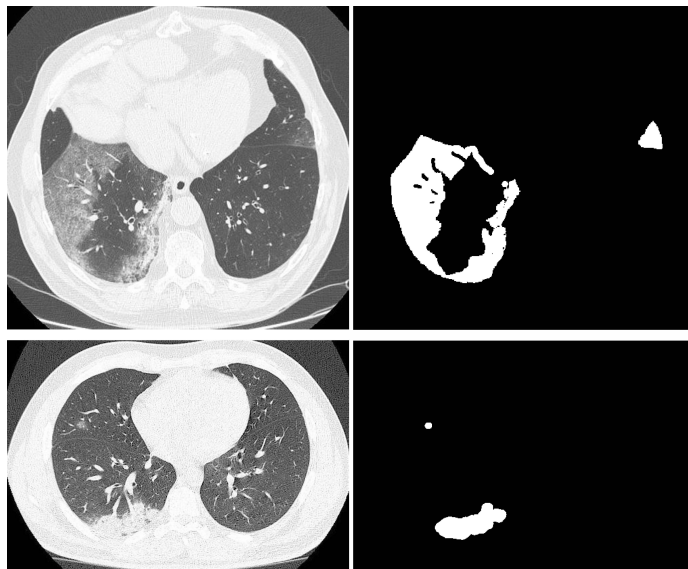


Figure 5: CT images from COVID-Seg dataset (first column) and the labeled masks of lesions (second column).

Method The total number of positive training images in COVID-CT and COVID-Seg is 467. Training deep learning models on such a small number of images is prone to overfitting. To address this issue, we incorporate additional information. In the COVID-Seg images, the regions containing COVID-19-related lesions are labeled with masks. These masks can inform the model to pay more attention to the lesion-containing regions. To incorporate these masks, we develop a multi-task learning framework that performs two tasks simulta-

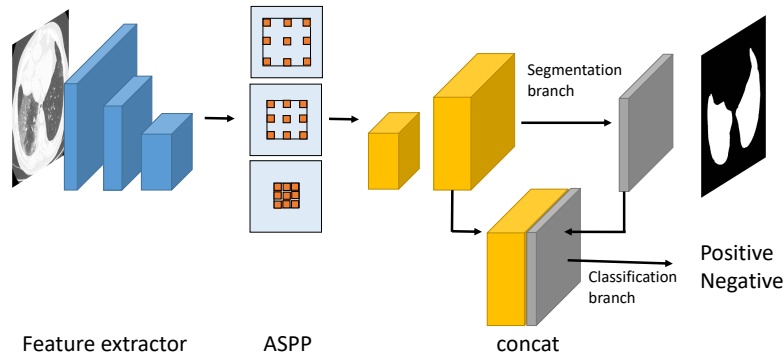


Figure 6: Architecture for joint classification and segmentation. The segmentation branch and the classification branch share the same feature extractor.

neously: segment out the regions containing lesions and classify the images as COVID-19 or non-COVID-19. The masks are used to supervise the learning of the segmentation task.

Figure 6 shows the architecture of the proposed joint classification and segmentation framework. During training, given a CT image, the network predicts the class label (whether this image is positive for COVID-19 or negative) and the lesion mask, by minimizing the sum of a classification loss and a segmentation loss. Given the image, we first use DenseNet-169 to extract visual features. Then the visual features are fed into an atrous spatial pyramid pooling (ASPP) (Chen et al., 2017) layer to extract denser and higher-resolution feature maps. These features maps are fed into two branches: a segmentation branch for predicting lesion segmentation mask and a classification branch for prediction class label. The predicted segmentation mask is fed into the classification branch as additional information. A segmentation loss function is defined between the groundtruth mask and predicted mask. A classification loss is defined between the groundtruth label and predicted label. The sum of these two losses are minimized for learning the weight parameters in the network. Note that the lesion masks are only required during training. During testing, the prediction is made solely based on test images and no lesion mask is required.

Experimental Settings In the multi-task learning framework, the weights associated with the segmentation loss and the classification loss are both set to 1. The rest of hyperparameter settings are the same as those in Section 3. We compare the following five methods: (1) DenseNet-169 on COVID-Seg; (2) DenseNet-169 on COVID-CT-349; (3) DenseNet-169 on the combination of COVID-Seg and COVID-CT-349 (Combination), which contains x images; (4) Joint classification and segmentation (JCS) on COVID-Seg; (5) JCS on Combination.

Results Table 5 shows the results of these five methods. From this table, we make the following observations. First, comparing JCS and DenseNet-169 on Combination, we can see that performing joint classification and segmentation can greatly improve performance. JCS on Combination achieves an accuracy of 83.3%, an F1 score of 84.6, and an AUC of 94.8%. This is because JCS incorporates additional supervision, which is the labeled regions of lesions, for model training. Second, JCS on Combination achieves substantially better

accuracy and F1 than JCS on COVID-Seg, which further demonstrates the usefulness of our COVID-CT dataset. Third, JCS on COVID-Seg works better than DenseNet-169 on COVID-Seg. This further shows the effectiveness of performing segmentation and classification jointly.

Method	Accuracy(%)	F1-score(%)	AUC (%)
DenseNet169 on COVID-Seg	64.8	50.0	79.5
DenseNet169 on COVID-CT-349	79.5	76.0	90.1
DenseNet169 on Combination	74.5	70.1	89.8
JCS on COVID-Seg	72.4	77.5	95.0
JCS on Combination	83.3	84.6	94.8

Table 5: Performance on the test set achieved by different methods.

5. Conclusions

We build a publicly available CT image dataset about COVID-19, to foster the development of AI methods for using CT to screen and test COVID-19 patients. The dataset contains 349 COVID-19 CT images from 216 patients and 463 non-COVID-19 CT images (used as negative training examples). The utility of this dataset is confirmed by a senior radiologist who has intensively practiced diagnosis and treatment of COVID-19 patients. We also perform experimental studies to further verify the utility of this dataset. Using this dataset, we develop a multi-task learning approach that achieves an F1 of 0.85, an AUC of 0.95, and an accuracy of 0.83, on a test set of original CT images donated by hospitals. For the next step, we will continue to improve the methods to achieve better accuracy.

References

- Liang-Chieh Chen, George Papandreou, Florian Schroff, and Hartwig Adam. Rethinking atrous convolution for semantic image segmentation. *arXiv preprint arXiv:1706.05587*, 2017.
- Jia Deng, Wei Dong, Richard Socher, Li-Jia Li, Kai Li, and Li Fei-Fei. Imagenet: A large-scale hierarchical image database. In *CVPR*, 2009.
- Gao Huang, Zhuang Liu, Laurens van der Maaten, and Kilian Q. Weinberger. Densely connected convolutional networks. In *The IEEE Conference on Computer Vision and Pattern Recognition (CVPR)*, July 2017.
- Lu Huang, Rui Han, Tao Ai, Pengxin Yu, Han Kang, Qian Tao, and Liming Xia. Serial quantitative chest ct assessment of covid-19: deep-learning approach. *Radiology: Cardiothoracic Imaging*, 2(2):e200075, 2020.
- Diederik P Kingma and Jimmy Ba. Adam: A method for stochastic optimization. *arXiv preprint arXiv:1412.6980*, 2014.

Lin Li, Lixin Qin, Zeguo Xu, Youbing Yin, Xin Wang, Bin Kong, Junjie Bai, Yi Lu, Zhenghan Fang, Qi Song, et al. Artificial intelligence distinguishes covid-19 from community acquired pneumonia on chest ct. *Radiology*, page 200905, 2020.